International Journal of Heat and Technology
Vol. 44, No. 3, June, 2026, pp. 1253-1270
Journal homepage: http://iieta.org/journals/ijht

Nano-Enhanced Phase Change Materials for Photovoltaic Cooling: A Meta-Analysis and Experimental Study of Paraffin–ZnO Thermal Regulation Performance

Mochamad Choifin, Zainal Arifin*, Ubaidillah, Budi Kristiawan

Department of Mechanical Engineering, Universitas Sebelas Maret, Surakarta, Jawa Tengah 57126, Indonesia

Corresponding Author Email: zainal_arifin@staff.uns.ac.id

https://doi.org/10.18280/ijht.440330

Received: 20 April 2026
Revised: 11 June 2026
Accepted: 18 June 2026
Available online: 30 June 2026

Keywords:
nano-enhanced phase change material, photovoltaic thermal management, meta-analysis, thermal conductivity enhancement, PV–PCM system performance

ABSTRACT

Thermal regulation remains a key limitation in photovoltaic (PV) systems because high operating temperatures reduce electrical efficiency and accelerate degradation. Nano-enhanced phase change materials (NePCMs) offer a promising solution by combining latent heat storage with improved thermal conductivity. This study investigates the thermal performance of NePCM for PV cooling through a combined meta-analysis and experimental validation approach. A systematic meta-analysis following the PRISMA 2020 framework was conducted using 30 peer-reviewed studies published between 2020 and 2025. Effect size analysis, heterogeneity evaluation, and publication bias assessment were performed. Experimental validation was then conducted using a laboratory PV system integrated with paraffin–ZnO NePCM containing 5 wt% ZnO nanoparticles to evaluate thermal and electrical performance under real solar irradiation. The meta-analysis revealed a pooled effect size of approximately 1.09, confirming a strong positive impact of nanoparticles on PCM thermal performance despite high heterogeneity ($I^2 \approx 83\%$). Experimentally, NePCM integration reduced the average PV temperature from 53.1 ℃ to 43.2 ℃, resulting in a 9.9 ℃ reduction and limiting thermal losses by about 40%. The improved thermal behavior from ZnO-enhanced PCM improves heat dissipation. It stabilizes PV operating temperature under high irradiance, demonstrating its effectiveness as a passive cooling strategy for improving PV thermal management and operational stability.

1. INTRODUCTION

Thermal energy storage (TES) has become an increasingly important technology for mitigating the intermittency of renewable energy systems, particularly those based on solar and wind resources. The integration of TES enables surplus thermal energy generated during peak production periods to be stored and subsequently utilized during periods of low energy availability, thereby improving overall system reliability and stability [1, 2]. Among the various TES technologies, latent heat storage using phase change material (PCM) has received significant scientific and engineering attention due to its high energy storage density and near-isothermal behavior during phase transitions. During the melting process, PCMs absorb large amounts of thermal energy, while during solidification, they release the stored heat, making them suitable for a wide range of thermal management applications [3, 4]. These applications include renewable energy systems, building thermal regulation, electronic cooling, and battery thermal management systems [5, 6].

Despite these advantages, the practical implementation of PCM-based TES systems is often hindered by the inherently low thermal conductivity of most commercially available PCMs. Organic PCMs such as paraffin waxes and fatty acids typically possess thermal conductivities in the range of 0.15–0.30 W/m·K, which is substantially lower than that of conventional heat transfer materials such as metals or even water [7, 8]. This low thermal conductivity results in slow heat transfer processes during both the melting and solidification stages. Consequently, PCM-based systems often experience prolonged charging and discharging durations, which can reduce their operational efficiency in real-world applications [7, 9, 10]. Furthermore, poor thermal conductivity leads to non-uniform temperature distributions within the storage medium, resulting in partial melting zones and inefficient utilization of the storage medium's latent heat capacity. These limitations significantly constrain the large-scale deployment of PCM-based thermal storage technologies in energy systems [11, 12].

To overcome these challenges, various thermal enhancement techniques have been developed and investigated in recent years, including nano-enhanced phase change materials (NePCMs). NePCMs are created by dispersing nanoscale particles with high thermal conductivity into a base PCM to enhance its overall thermophysical properties. Various nanoparticles have been explored in the literature, including metal oxides such as Al_2O_3, CuO, TiO_2, and ZnO, pure metals such as Cu and Ag, and carbon-based nanomaterials such as graphene, graphene oxide, carbon nanotubes, and expanded graphite [13, 14]. These nanoparticles act as conductive pathways within the PCM matrix, facilitating faster heat transfer and improving the thermal response of the storage system. As a result, NePCMs can significantly reduce melting time, improve heat distribution, and increase the composite material's effective thermal conductivity [15, 16].

The thermal performance of NePCMs is strongly influenced by the morphological characteristics of the nanoparticles, as well as their concentration and dispersion stability within the PCM matrix [15, 17]. Adding nanoparticles generally increases PCM thermal conductivity and accelerates melting/solidification, reducing charging/discharging times [18, 19]. Previous studies have demonstrated the effectiveness of integrating PCM and nanomaterials in improving the thermal management of energy systems. As summarized in Table 1, numerous experimental, numerical, and review-based investigations have evaluated the performance of photovoltaic thermal (PVT) systems incorporating PCM. Several investigations have reported improvements in thermal efficiency exceeding 60%, while reductions in PV operating temperature exceeding 20 ℃ have also been documented [20, 21]. The results further indicate that hybrid cooling strategies combining PCM with nanofluids or porous conductive matrices offer substantial improvements in heat dissipation performance. Such findings highlight the important role of thermally enhanced PCM systems in next-generation renewable energy technologies.

Despite these advancements, existing research on NePCM-based thermal enhancement in photovoltaic (PV) systems remains fragmented and methodologically inconsistent. Table 1 shows that many previous studies report the performance of PVT when relying on specific configurations, such as higher thermal efficiencies by upwards of 60%, with some articles mentioning electrical efficiencies naturally increasing in the range of 2–10%, and a suggested decrement in temperature over PV types typically limited to an approximate reduction of 16–26 ℃. In addition, many studies focus on numerical modeling or experimental assessment in isolation rather than through a systematic synthesis of accumulating evidence. However, this creates an important gap in the development of standard performance metrics for consistent comparison across studies, limiting the generalizability of design principles when integrating NePCM components into PV thermal-regulating systems.

To overcome the limitation, this study provides a more robust and integrative methodology that combines a meta-analysis with controlled experimental validation using a paraffin–ZnO NePCM system. In contrast with previous studies that focus on single-method investigations, this dual-framework approach allows both macroscopic quantification of global research tendencies and microscopic validation in controlled laboratory environments. The meta-analysis delivers a statistically meaningful effect-size estimate across 30 studies, enabling NePCM systems to be benchmarked against the current literature. At the same time, the experimental part substantiates these aggregated findings by subjecting real PV devices to solar irradiation. The integration greatly improves methodological robustness, allowing results to be reported in the context of prior results as relative percentiles and enabling direct comparison between current and prior PVT–PCM studies. Thus, while the study substantiates its findings by showing why ZnO–paraffin NePCM is better for lowering PV operating temperature and improving efficiency relative to conventional thermally conductive materials, it also moves the scientific field forward by providing an integrated framework integrating data from literature synthesis with experimental validation into a unified concept of PV thermal management research.

Table 1. Research summary of PCM and nanomaterial integration in PVT thermal management systems

Reference	Approach / Method	Research Focus	Key Findings
[22]	Experimental PVT system using nano-emulsion PCM coolant	Performance evaluation of PVT systems with nano-PCM-based cooling	Nano-emulsion PCM enhanced thermal energy efficiency up to 89.23% compared with conventional water cooling systems
[23]	Experimental study of PVT system with nano-PCM and twisted absorber tube	Investigation of nanoparticle-enhanced PCM effects in PVT collectors	Total system efficiency reached 94.31%, showing significant improvement in thermal performance
[24]	Multiphysics CFD simulation with experimental validation	Development of a CFD model for a PVT system with perforated fins and PCM	Heat dissipation improved by 28.3%, PV temperature decreased by 16.1 ℃, and energy output increased by 9.2%
[25]	3D CFD modeling of PVT-PCM system with wavy fins	Optimization of fin configuration and airflow structure in PVT systems	Thermal efficiency increased by 61.35%, while electrical efficiency improved by 2%
[26]	Experimental hybrid cooling system (nanofluid + finned PCM)	Effect of nanofluid and PCM integration in CPV-T systems	PV module temperature decreased by 26.6 ℃, and electrical efficiency improved to 17.02%
[27]	Outdoor experimental PVT-PCM system with nanofluid	Energy, exergy, economic, and environmental performance analysis	Thermal output increased by 44.54%, and energy cost savings reached 19.63% compared with conventional PV systems
[28]	Comparative experimental study (PCM, TEG, nanofluid cooling)	Evaluation of different PVT cooling technologies	Cell temperature reduced by more than 20%, while electrical efficiency reached 15.5%
[29]	Experimental and numerical investigation of PVT with PCM and metal foam	Integration of PCM with copper foam matrix to enhance thermal conductivity	Thermal efficiency increased up to 72.74% with an electrical efficiency improvement of 10.74%
[30]	Experimental and simulation study of PVT with dual-parallel cooling channels and PCM	Optimization of PCM thickness and coolant flow rate	The system effectively reduced PV temperature and improved thermal energy stability
[31]	Systematic review of PVT-PCM systems	Assessment of the development of PCM integration in PVT technologies	PCM significantly improves PV thermal management and contributes to longer module lifespan

Note: PV = photovoltaic; PVT = photovoltaic thermal; PCM = phase change material.

2. METHOD

2.1 Meta-analysis and experimental validation framework

This study adopts a two-stage methodological framework integrating meta-analysis with experimental validation to systematically investigate the thermal performance of NePCM in PV systems. The first stage focuses on a comprehensive synthesis of existing literature using a structured meta-analysis approach guided by the Preferred Reporting Items for Systematic Reviews and Meta-Analyses (PRISMA) 2020 framework [32-34]. The overall research workflow is illustrated in Figure 1, which presents the conceptual research process and the systematic procedure for selecting relevant studies. As shown in Figure 1(a), the research begins with an extensive literature review to identify scientific studies on PCM enhancement, nanoparticle integration, and PV thermal management. This initial stage establishes the theoretical and analytical foundation for the research by systematically compiling empirical findings from previous studies. The integration of structured literature synthesis with quantitative evaluation ensures that the research is grounded in a comprehensive understanding of existing scientific evidence.

The literature search was conducted across several major scientific databases, including Scopus, Web of Science, ScienceDirect, Google Scholar, and IEEE Xplore, to ensure comprehensive coverage of peer-reviewed publications relevant to NePCM thermal performance. The search was conducted in December 2025 and covered publications from January 2020 to December 2025. The search strategy employed a combination of controlled vocabulary terms and free-text keywords, connected by Boolean operators, to maximize the retrieval of relevant studies across multiple research disciplines. The primary Boolean search string used in the database queries was ("nano-enhanced phase change material*" OR "NePCM" OR "NEPCM" OR "nanoparticle* enhanced PCM" OR "nano-PCM" OR "nanofluid PCM") AND ("thermal conductivity" OR "thermal performance" OR "heat transfer" OR "latent heat" OR "melting" OR "solidification" OR "phase change" OR "3vometer3t*" OR "characterization") AND ("nanoparticle*" OR "3vometer3ture*" OR "graphene" OR "carbon nanotube*" OR "Al_2O_3" OR "CuO" OR "TiO_2" OR "ZnO"). Additional relevant studies were identified through manual screening of the reference lists of selected articles and review papers to ensure that potentially significant studies were not omitted from the dataset. The collected literature was subsequently evaluated using quantitative analytical tools, such as forest plots, funnel plots, risk-of-bias assessments, and effect-size analyses, to identify research trends and quantify the magnitude of thermal performance improvements reported in previous studies.

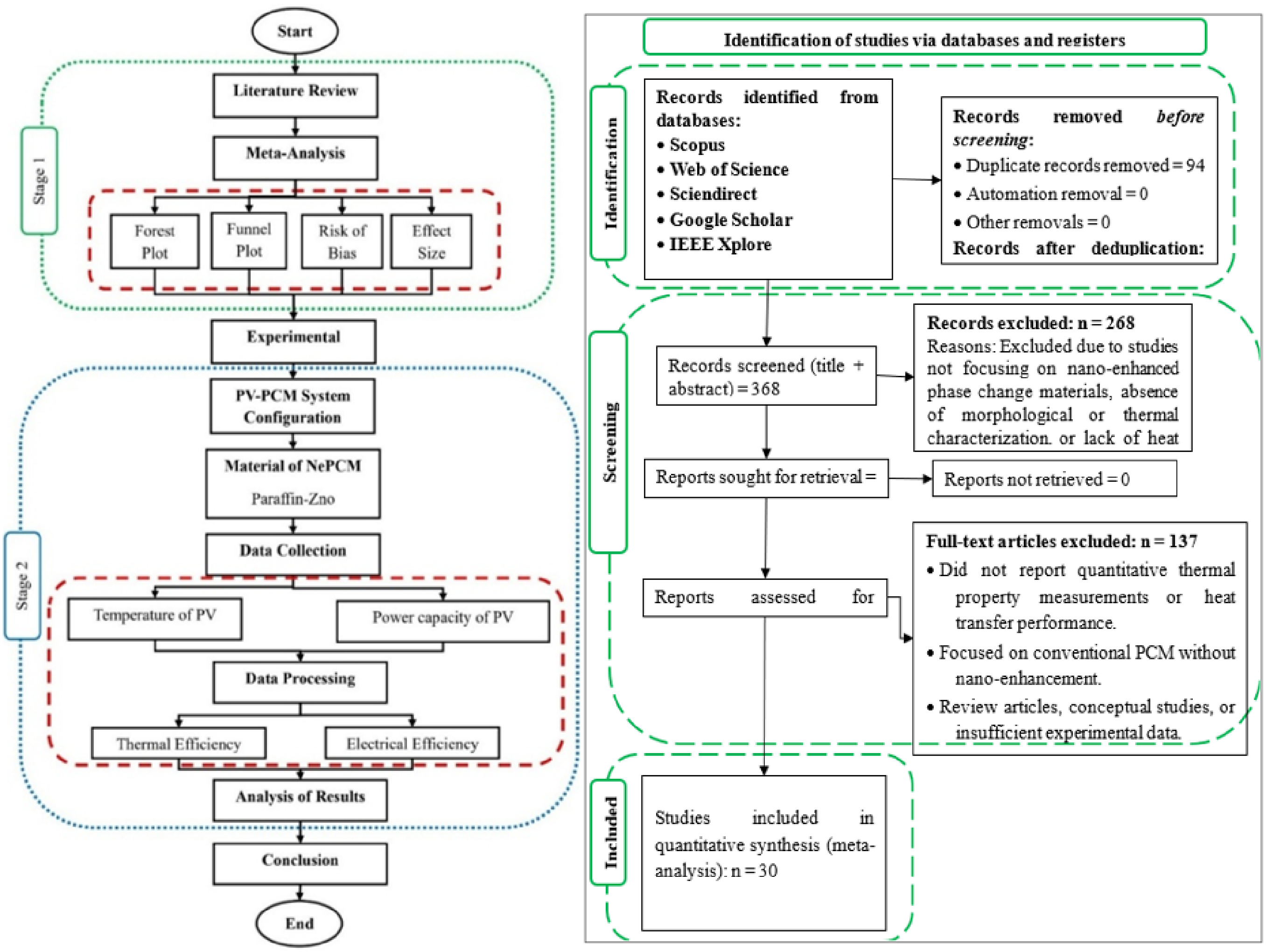

(a) (b)

Figure 1. Integrated research methodology (a) Flow diagram of research and (b) Preferred Reporting Items for Systematic Reviews and Meta-Analyses (PRISMA) 2020 literature selection process

The second stage of the methodology focuses on experimental validation designed to evaluate the thermal performance of NePCM within a PV–PCM configuration using paraffin–ZnO as the composite material. The experimental procedure begins with the configuration of the PV–PCM system, followed by the preparation of NePCM materials comprising paraffin integrated with ZnO nanoparticles. The selection of paraffin as the base PCM is based on its favorable thermophysical properties, including stable melting behavior and a relatively high latent heat storage capacity. ZnO nanoparticles are incorporated into the PCM matrix to enhance thermal conductivity and improve heat transfer performance within the storage medium. The preparation of NePCM is conducted using controlled dispersion techniques to ensure homogeneous distribution of nanoparticles within the paraffin matrix. This preparation step is essential to maintain the stability and reliability of the thermal performance during the experimental evaluation.

Subsequently, systematic data collection is conducted by monitoring two principal parameters: PV temperature and PV power capacity, which directly influence the PV system's thermal behavior and electrical performance. The collected experimental data are processed to determine thermal efficiency and electrical efficiency as the primary indicators of system performance. In parallel with the experimental workflow, the systematic literature screening process used in the meta-analysis stage follows the procedure illustrated in Figure 1(b) based on the PRISMA 2020 framework. The screening procedure consists of identification, screening, eligibility evaluation, and final inclusion stages based on predefined inclusion and exclusion criteria. Through this systematic selection process, 30 studies were included in the quantitative synthesis for the meta-analysis. The integration of large-scale literature synthesis with experimental validation provides a robust methodological foundation, enabling the study to establish a strong relationship between statistical evidence derived from previous research and empirical verification obtained from the experimental investigation.

2.2 Data extraction and coding

Data extraction was conducted systematically to ensure consistency and reproducibility across all selected studies included in the meta-analysis. The extraction process was performed independently by two reviewers using a standardized coding form to minimize potential bias and discrepancies in data interpretation. For each included study, several categories of information were collected, including bibliographic details such as authors, publication year, journal source, and country of origin. In addition, study characteristics were documented, including whether the study employed experimental, numerical, or combined methodologies as well as the reported sample size. Detailed nanoparticle specifications were also extracted, including nanoparticle type, dimensionality, particle size, shape, and any reported surface modification treatments used to enhance dispersion within the PCM matrix. Information regarding the base PCM was also recorded, including the type of PCM used, its melting temperature, and baseline thermal conductivity. Furthermore, details of the NePCM preparation process were documented, including sonication duration, surfactant type and concentration, and the mixing protocols used to achieve homogeneous nanoparticle dispersion.

Additional variables extracted from the literature included nanoparticle concentration expressed either as weight percentage or volume fraction, as well as characterization techniques used to evaluate the structural and thermophysical properties of the materials. Common characterization methods reported in the selected studies included Differential Scanning Calorimetry (DSC), Scanning Electron Microscopy (SEM), Transmission Electron Microscopy (TEM), X-ray Diffraction (XRD), Thermogravimetric Analysis (TGA), and laser flash analysis. Outcome variables and statistical indicators were also extracted, including mean values, standard deviations, percentage improvements, and confidence intervals associated with thermal performance indicators. For studies evaluating thermal conductivity enhancement, numerical values were extracted for both pure PCM (control group) and NePCM (treatment group) conditions to allow direct comparison. When multiple nanoparticle concentrations were reported within a single study, each concentration level was treated as an independent comparison in the dataset to preserve the granularity of the experimental observations. When standard deviations were not explicitly reported in the original study, they were estimated from standard errors, confidence intervals, or reported data ranges following established methodological guidelines.

The primary effect size metric used in the meta-analysis was the standardized mean difference (SMD), commonly expressed as Cohen's d, which quantifies the magnitude of improvement between the NePCM system and the baseline PCM condition. The SMD was calculated using the difference between the mean thermal property values of the treatment and control groups, normalized by the pooled standard deviation. The formula used for calculating the SMD is expressed as Eq. (1) [35]:

$$SMD = \frac{\bar{X}_{NePCM} - \bar{X}_{PCM}}{S_p} \tag{1}$$

where, $\bar{X}_{NePCM}$ represents the mean value of the NePCM group, $\bar{X}_{PCM}$ represents the mean value of the pure PCM group, and S_p represents the pooled standard deviation of both groups. The pooled standard deviation is calculated as in Eq. (2) [36, 37]:

$$S_p = \sqrt{\frac{(n_1 - 1)S_1^2 + (n_2 - 1)S_2^2}{n_1 + n_2 - 2}} \tag{2}$$

where, S_1 and S_2 represent the standard deviations of the treatment and control groups, and n_1 and n_2 denote the respective sample sizes.

2.3 Quality assessment and risk of bias

The methodological quality and risk of bias of the included studies were evaluated using a modified version of the Cochrane Risk of Bias framework, specifically adapted for materials science and engineering research contexts. This modified framework enables a structured evaluation of potential methodological limitations that may influence the reliability of the reported results. Seven assessment domains were evaluated to capture different potential sources of bias. The first domain focused on bias in the selection of reported measurements, evaluating whether outcome variables were clearly predefined or selectively reported after data analysis. The second domain assessed bias in the measurement of thermal properties by evaluating the calibration procedures of measurement instruments, the standards used in the experiments, and the accuracy of the measurement techniques. The third domain examined potential bias in morphological characterization, particularly evaluating whether sufficient structural analysis using techniques such as SEM, TEM, or XRD was conducted to confirm nanoparticle dispersion and structural integrity.

Additional domains included bias in the experimental procedures and protocols, which assessed the clarity and reproducibility of the methodologies used in each study. Bias in data analysis and reporting was also evaluated, focusing on whether appropriate statistical methods were used and whether the reported data were sufficiently complete to support the conclusions. Another important domain assessed the consistency of sample preparation, evaluating whether the studies reported batch-to-batch variability and quality control procedures during NePCM preparation. Based on the evaluation of these domains, each study was classified as having low risk, some concerns, or high risk of bias. The final domain represented an overall assessment of risk of bias, which combined the outcomes of the previous domains to provide a holistic evaluation of the methodological quality of each study.

2.4 Statistical methods for meta-analysis

The meta-analysis used both fixed- and random-effects models to evaluate the aggregated thermal performance improvements of NePCM systems. The fixed-effect model employed inverse variance weighting, assuming that all included studies estimate a common true effect size. However, due to expected variability in nanoparticle types, concentration ranges, PCM materials, and experimental conditions, the random-effects model based on the DerSimonian–Laird method was selected as the primary analytical framework. This model accounts for both within-study sampling error and between-study heterogeneity, thereby producing more conservative and generalizable pooled estimates. All statistical analyses and data processing procedures were implemented in Python 3.10, using scientific computing libraries for statistical modeling and data visualization.

Heterogeneity among studies was evaluated using several complementary statistical indicators, including Cochran's Q test, the I^2 statistic, and between-study variance τ^2. Cochran's Q statistic tests whether the variation in observed effect sizes across studies exceeds what would be expected from random sampling error alone. The mathematical expression for Cochran's Q statistic is given as Eq. (3) [38, 39]:

$$Q = \sum_{i=1}^{k} w_i \, (E_i - \bar{E})^2 \qquad (3)$$

where, w_i represents the inverse variance weight for the study i , E_i represents the individual study effect size, and $\bar{E}$represents the pooled effect estimate across all studies. To quantify the proportion of variability attributable to heterogeneity rather than sampling error, the I^2 statistic is calculated using the following Eq. (4) [40]:

$$I^2 = \frac{Q - df}{Q} \times 100\% \qquad (4)$$

where, $df = k - 1$ represents the degrees of freedom and $k$represents the total number of included studies. Values of I^2 equal to 25%, 50%, and 75% are commonly interpreted as low, moderate, and high heterogeneity, respectively.

Publication bias was evaluated using visual inspection of funnel plots and formal statistical tests, including Egger's regression test and the Begg–Mazumdar rank correlation test. Funnel plots examine the relationship between effect sizes and their corresponding standard errors to identify asymmetry that may indicate publication bias. When evidence of bias was detected, the trim-and-fill method was applied to estimate the number of potentially missing studies and to adjust the pooled effect estimate accordingly. In addition, subgroup analyses were conducted to explore potential sources of heterogeneity by grouping studies according to nanoparticle type, dimensionality, concentration range, PCM type, and study design. Sensitivity analyses were also conducted, including leave-one-out analysis and influence diagnostics, to assess the robustness and stability of the overall meta-analysis results.

2.5 Experimental configuration and performance evaluation of the photovoltaic–nano-enhanced phase change material system

To experimentally evaluate the thermal and electrical performance of PV–NePCM, a laboratory-scale experimental configuration was developed as illustrated in Figure 2. The system consists of a PV module mounted on an inclined support structure with a NePCM layer attached to the rear surface of the PV panel to enhance heat absorption and thermal regulation. Solar irradiation serves as the primary heat source, while heat transfer mechanisms, including radiation and natural convection, occur at both the front and rear surfaces of the PV module. During operation, the NePCM layer absorbs excess heat generated by the PV panel during peak solar exposure, thereby limiting temperature rise in the PV cells and stabilizing their operating temperature. Measurement devices, including a data logger and an 5vometer, were connected to the PV module to record temperature and electrical output parameters. At the same time, a laptop was used for data acquisition and post-processing.

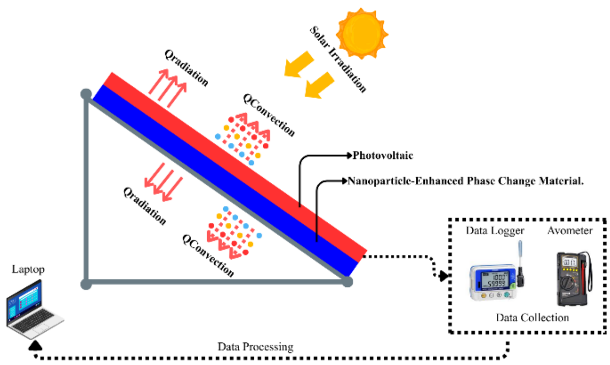

Figure 2. Schematic illustration of the experimental configuration of the photovoltaic–phase change material (PV–PCM) system used for thermal and electrical performance evaluation

The integration of NePCM with the PV module is critical for passive thermal management. As the PV surface absorbs solar radiation, a portion of the energy is converted into electricity, while the remaining fraction is dissipated as heat, increasing the PV cells' temperature. Elevated temperatures negatively affect PV efficiency by increasing carrier recombination and reducing voltage output. By incorporating

NePCM on the backside of the PV module, excess thermal energy can be stored as latent heat during melting, thereby reducing the rate of temperature increase in the PV layer. This thermal buffering mechanism improves the stability of PV operation under fluctuating solar irradiance and enhances overall energy utilization in the PV–NePCM system.

To quantitatively evaluate the thermal performance of the system, the thermal efficiency of the PV–NePCM configuration can be estimated based on the temperature difference between the PV surface and the ambient environment. Thermal efficiency represents the ability of the system to dissipate or store absorbed heat and can be expressed as Eq. (5) [6, 16]:

$$\eta_{th} = \frac{hA(T_{pv} - T_{amb})}{GA} \quad (5)$$

where, η_{th} represents the thermal efficiency, h is the convective heat transfer coefficient, A is the surface area of the PV module, T_{pv} is the measured temperature of the PV module, T_{amb} is the ambient temperature, and Grepresents the incident solar irradiance. In this study, the active surface area of the PV module was determined based on the panel dimensions of 0.65 × 0.54 m, resulting in a total area of A = 0.351 m^2. This formulation relates the heat rejected from the PV surface to the total incoming solar energy and provides an indicator of the PV–NePCM system's thermal management capability.

In addition to thermal performance, the electrical efficiency of the PV module was evaluated using the measured electrical output power. Electrical efficiency describes the fraction of incident solar radiation that is converted into usable electrical energy and is calculated using the following Eq. (6) [8, 41, 42]:

$$\eta_{el} = \frac{P_{out}}{GA} \quad (6)$$

where, η_{el} represents the electrical efficiency of the PV module, P_{out} is the PV panel generating the electrical output power, G is the solar irradiance, and A is the active surface area of the PV module. By combining both thermal and electrical performance indicators, the PV–NePCM experimental configuration provides a comprehensive framework for evaluating the effectiveness of NePCM-based thermal management strategies in improving PV energy conversion performance.

3. RESULT

3.1 Stage 1

3.1.1 Nanoparticle morphology and thermal conductivity enhancement in nano-enhanced phase change materials systems

The compiled dataset of NePCM studies shows significant variability in thermal conductivity enhancement across nanoparticle type, concentration, and preparation method. As summarized in Table 2, the analyzed studies include a range of nanoparticle materials such as CuO, Al_2O_3, carbon-based nanomaterials, and expanded graphite integrated with different PCM matrices, including paraffin wax, octadecane, and fatty acid-based PCM. The concentration of nanoparticles used across studies ranges from very low loading fractions of approximately 0.3 wt% to higher concentrations of 20 wt%, indicating the wide range of experimental conditions reported in the literature. In general, metal oxide nanoparticles, such as CuO and Al_2O_3, exhibit measurable increases in thermal conductivity and are widely used in solar energy cooling applications. In addition to these two types of nanoparticles, other types, such as ZnO, remain to be fully explored. Therefore, this study will focus on exploring ZnO-based NePCM as a cooling medium for solar panels.

Table 2. Summary of nanoparticle–phase change material (PCM) compositions and thermal conductivity performance in selected nano-enhanced phase change material (NePCM) studies

Study	Nanoparticle Type	Base PCM	Conc. (wt%)	Thermal Conductivity	Study Method
[43]	CuO nanoparticles	Paraffin (Octadecane)	1–2	22.6	Numerical Simulation
[44]	CuO nanoparticles	Paraffin wax	0.3–1.2	24.9	Experimental
[45]	Al_2O_3 nanoparticles	Paraffin wax	4–11	0.307	Experimental
[46]	Al_2O_3 nanoparticles	Paraffin wax	1–10	0.466	Experimental
[47]	Al_2O_3 nanoparticles	Paraffin wax	1	13	Experimental
[48]	Al_2O_3 nanoparticles	Binary fatty acid PCM	1–5	0.40	Experimental
[49]	Al_2O_3 nanoparticles	Beeswax PCM	2–8	0.38	Experimental
[50]	Carbon quantum dots	Paraffin wax	1–20	0.35	Experimental
[51]	Expanded graphite nanostructure	Paraffin PCM	5	0.60	Experimental
[52]	CuO-functionalized nanofibers	Paraffin PCM	3	25	Numerical Simulation

Table 3. Morphological classification and thermal performance characteristics of nanoparticles in nano-enhanced phase change material (NePCM) systems

Dimension	Examples	Size Range	TC Enhancement	LH Impact	Key Mechanism
0D (Spherical)	Al_2O_3, CuO, TiO_2, ZnO, SiO_2	10–50 nm dia.	59–195%	-5 to -15%	Phonon scattering
1D (Tubular/Fibrous)	CNT, MWCNT, SiC NW, Carbon fiber	5–30 nm dia., 1–25 µm length	240–377%	-8 to -20%	Thermal bridges
2D (Planar)	Graphene, GO, rGO, h-BN, MXene	0.1–10 µm lateral, 0.3–5 nm thick	421–720%	-10 to -25%	Planar conduction
3D (Porous)	EG, Metal foam, MOF, Tetrapods	µm–mm pore size	1287–2696%	-15 to -61%	Porous network
Hybrid	CNT + GNP, GO + BN, Ag-Graphene	Multi-scale	308–950%	-8 to -30%	Synergistic effects

In addition, both experimental investigations and numerical simulations consistently show that integrating nanoparticles into paraffin-based PCM can significantly accelerate heat transfer during melting and solidification cycles. These findings collectively indicate that nanoparticle-enhanced PCM systems offer a promising approach to improving the thermal response of TES systems, particularly when nanoparticle morphology and dispersion quality are carefully controlled.

In addition to nanoparticle type and concentration, nanoparticle morphology also plays a crucial role in determining the thermal performance of NePCM systems. The classification of nanoparticle structures into zero-, one-, two-, and three-dimensional categories provides a useful framework for understanding the mechanisms governing thermal transport enhancement. As shown in Table 3, spherical nanoparticles, categorized as 0D materials, primarily enhance heat transfer via localized phonon scattering and isotropic conduction pathways within the PCM matrix. In contrast, 1D nanostructures, such as carbon nanotubes, create elongated conductive channels that act as thermal bridges, significantly increasing heat transfer efficiency throughout the material. Two-dimensional nanomaterials, including graphene and graphene oxide, provide extensive planar contact surfaces that enhance interfacial heat transfer between the nanoparticles and the surrounding PCM. Meanwhile, three-dimensional porous structures such as expanded graphite form interconnected conductive networks that enable rapid heat distribution throughout the composite material. Hybrid nanoparticle systems combining multiple structural dimensions further demonstrate synergistic effects that can simultaneously enhance thermal conductivity while maintaining acceptable latent heat capacity [17, 53].

The addition of nanoparticles to PCM generally increases thermal conductivity, thereby accelerating the heat storage and release processes due to improved thermal performance within the material matrix; however, increasing the nanoparticle concentration does not always result in a linear improvement in performance, as excessively high concentrations can disrupt the PCM structure, leading to a decrease in latent heat and changes in thermophysical properties such as melting point and degree of supercooling, thus creating a trade-off between enhanced heat transfer and reduced energy storage capacity [54]. Various studies indicate that there is an optimal concentration of nano-PCM that must be maintained to ensure long-term stability of thermal properties, beyond which system performance may actually decline due to degradation of phase-change characteristics. In PV–nano-PCM applications, experimental results also indicate that decreases in module temperature and increases in efficiency do not occur at the highest concentrations tested (0.5–7.5 wt%), but rather at specific, more precise concentrations [55-57]. Numerical modeling of the PVT system shows that, under certain weather conditions, thermal performance improvements are optimal at lower nanoparticle concentrations, confirming that the effectiveness of nano-PCM is highly dependent on concentration optimization and environmental operating conditions [58].

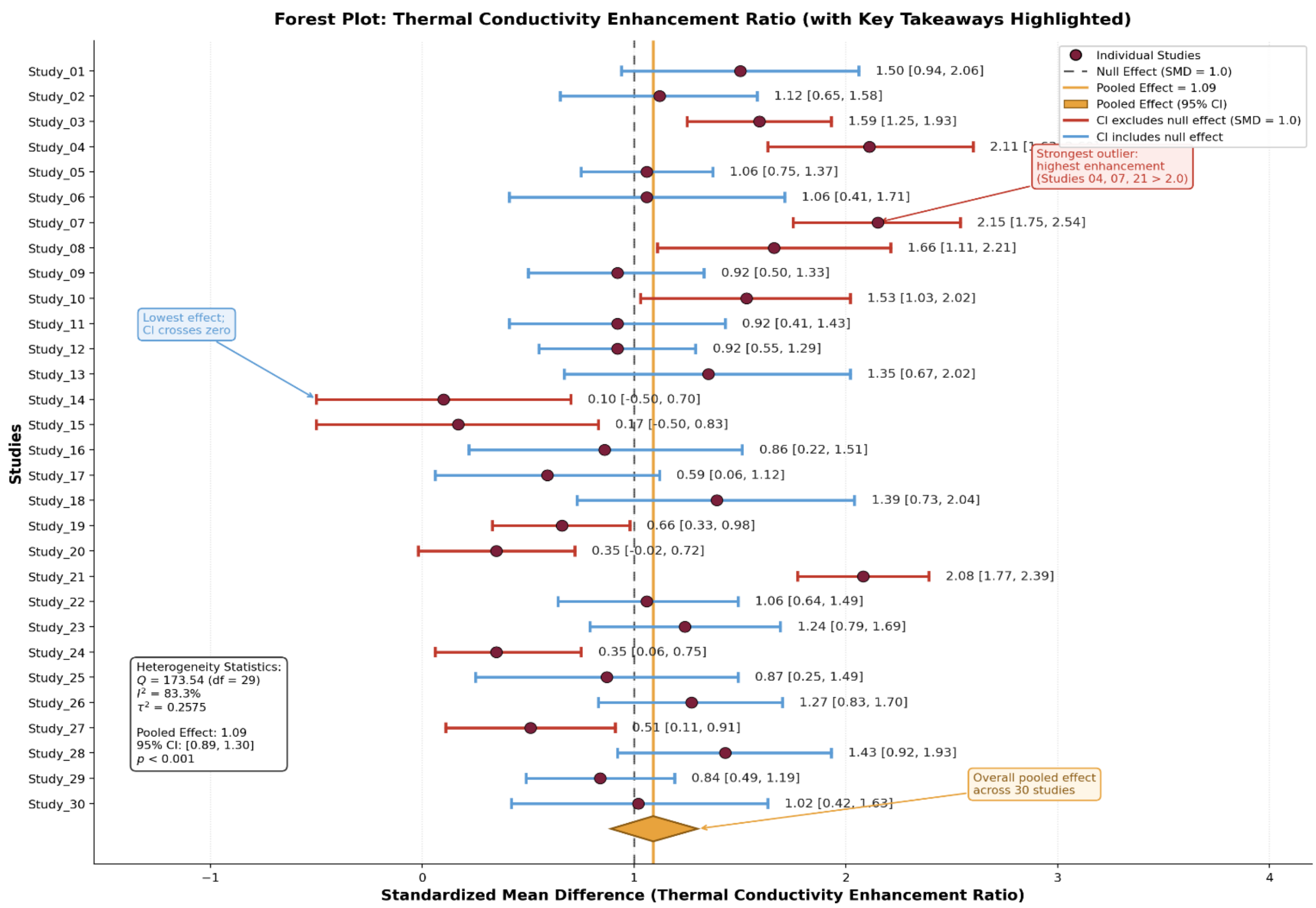

Figure 3. Forest plot of effect size distribution and heterogeneity in nano-enhanced phase change material (NePCM) thermal performance studies

3.1.2 Meta-analysis results of Nano-enhanced phase change materials thermal performance and bias evaluation

The quantitative synthesis of the NePCM dataset reveals a consistently positive effect of nanoparticle incorporation on the thermal performance of PCM systems across the analyzed literature. Based on the meta-analysis results, the pooled effect size from the random-effects model is approximately 1.0942, indicating a significant improvement in thermal properties when nanoparticles are incorporated into PCM matrices. The confidence interval for the pooled effect ranges from 0.8920 to 1.2964, suggesting that the enhancement effect is statistically robust across the majority of included studies. The distribution of individual study effect sizes ranges from 0.1000 to 2.1475, reflecting substantial variability in the magnitude of reported performance improvements across nanoparticle morphology, concentration, and experimental configurations. The statistical heterogeneity analysis corroborates this interpretation, revealing a high degree of between-study variability with an I^2 value of approximately 83.29%. This level of heterogeneity indicates that a substantial proportion of the observed variation in effect sizes is not attributable to random sampling error, but rather to real differences in experimental setups, material compositions, and operational conditions. Consequently, the findings suggest that thermal performance outcomes in nanoparticle-enhanced systems are strongly influenced by study-specific parameters, underscoring the necessity of standardized methodologies and controlled comparative frameworks to isolate the true effect of nanoparticle integration more accurately. Furthermore, Cochran's Q statistic confirms that the variation among study results exceeds what would be expected from sampling error alone [14, 46]. The distribution of effect sizes and the presence of several outlier studies are illustrated in Figure 3, which demonstrates that although most studies report positive thermal enhancement, the magnitude of improvement varies considerably across different NePCM configurations.

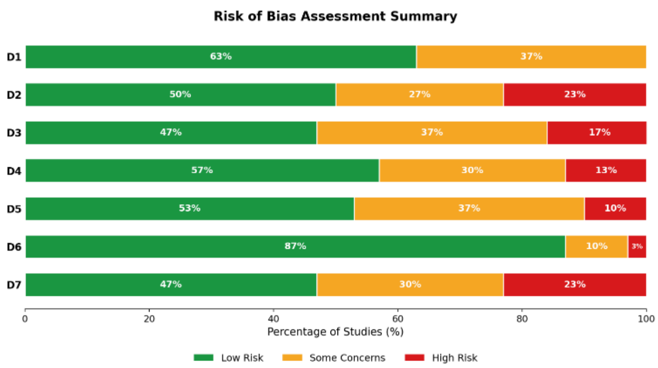

Figure 4. Risk of bias distribution across seven assessment domains in nano-enhanced phase change material (NePCM) studies

In addition to evaluating thermal performance improvements, the reliability of the analyzed studies was assessed using a structured risk-of-bias assessment across seven methodological domains. The assessment results indicate that the overall quality of the included studies is generally acceptable, with approximately 53.3% categorized as low risk and 46.7% classified as having some concerns. Importantly, none of the evaluated studies were classified as having an overall high risk, suggesting that the majority of the reported experimental procedures and analytical methods are methodologically sound. Domain-specific analysis shows that the lowest level of bias is observed in the "Other Bias" category, where most studies demonstrate adequate control of external experimental variables. In contrast, moderate levels of concern appear in domains related to allocation procedures and blinding, which are commonly challenging to implement in materials science experiments involving laboratory-scale thermal characterization [53, 59]. The seven evaluated domains include D1: Randomization, D2: Allocation Concealment, D3: Blinding, D4: Incomplete Data, D5: Selective Reporting, D6: Other Bias, and D7: Overall Bias. The overall distribution of methodological quality across these domains is summarized in Figure 4, which provides a comprehensive overview of the reliability and reproducibility of the studies included in the meta-analysis.

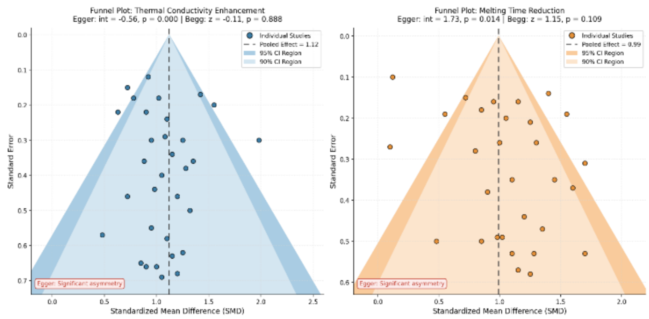

Figure 5. Funnel plot distribution for thermal conductivity enhancement across nano-enhanced phase change material (NePCM) studies

3.1.3 Publication bias evaluation and subgroup analysis of thermal performance in NePCM systems

The funnel plot analysis provides an important diagnostic evaluation of potential publication bias and distribution symmetry in the meta-analysis dataset related to thermal conductivity enhancement in NePCM systems. The aggregated statistical results indicate that the pooled effect size from the random-effects model is approximately 1.1222, with a confidence interval of 0.9270 to 1.3174, suggesting a consistent improvement in thermal conductivity when nanoparticles are incorporated into PCM matrices. However, the heterogeneity analysis reveals moderate to high variability among the included studies, with an I^2 value of approximately 69.41%, indicating that experimental conditions, nanoparticle morphology, and preparation techniques contribute significantly to the observed variation in reported thermal performance. The statistical assessment of publication bias shows mixed results: the Egger's regression test suggests potential asymmetry in the dataset, while the Begg rank correlation test indicates no statistically significant bias. This discrepancy is commonly observed in meta-analytical studies involving relatively small sample sizes and heterogeneous experimental conditions [60, 61]. The distribution of studies in the funnel plot indicates that approximately 76.7% of the included studies fall within the expected confidence boundaries, while a smaller proportion are classified as outliers. The graphical representation of this distribution pattern is shown in Figure 5, which illustrates the spread of effect sizes relative to their associated standard errors.

Beyond evaluating thermal conductivity enhancement alone, the complete meta-analysis dataset also provides insights into several additional thermal performance indicators associated with NePCM systems. These indicators include latent heat variation, melting behavior, enhanced heat transfer coefficient, and supercooling characteristics, which collectively influence the overall thermal performance of PCM-based energy storage systems. The dataset reveals that most studies report positive thermal conductivity enhancement and improved heat transfer performance. In contrast, latent heat generally decreases slightly due to the introduction of nanoparticles into the PCM matrix. This reduction is expected because the addition of solid nanoparticles partially replaces the volume of the active phase-change material, thereby slightly decreasing the available latent heat storage capacity [62, 63]. However, improvements in heat transfer rates and reductions in melting time often compensate for this minor decrease in latent heat, resulting in an overall enhancement in system performance. The combined distribution of effect sizes across these different thermal indicators is presented in Figure 6, which illustrates the multidimensional impact of nanoparticle incorporation on the thermal behavior of NePCM systems.

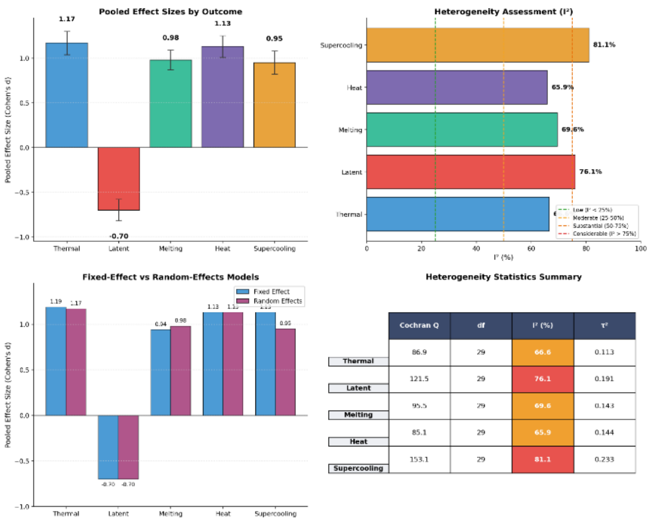

Figure 6. Comparative effect size distribution for multiple thermal performance indicators in nano-enhanced phase change material (NePCM) studies

Further insights into the factors influencing NePCM performance can be obtained through subgroup analysis based on nanoparticle type and concentration. The results indicate that metal oxide nanoparticles, such as Al_2O_3 and CuO, exhibit relatively strong thermal enhancement effects, with pooled effect sizes exceeding 1.40, suggesting that these materials provide effective conductive pathways within the PCM matrix. In contrast, several other nanoparticle categories, such as TiO_2, Cu, and carbon-based nanotube materials, exhibit comparatively lower enhancement levels, which may be attributed to differences in particle morphology, dispersion stability, and interfacial thermal resistance [64, 65]. The concentration-based subgroup analysis also reveals that lower nanoparticle concentrations, approximately 0.1–0.5 wt%, tend to yield the most consistent thermal conductivity improvements. Increasing nanoparticle concentration beyond this range does not always lead to proportional performance enhancement due to potential particle agglomeration and increased viscosity within the composite material. These findings highlight the importance of optimizing both nanoparticle selection and concentration levels to achieve balanced thermal performance in NePCM systems. The comparative results of these subgroup analyses are summarized in Figure 7, which shows variation in pooled effect sizes across nanoparticle categories and concentration ranges.

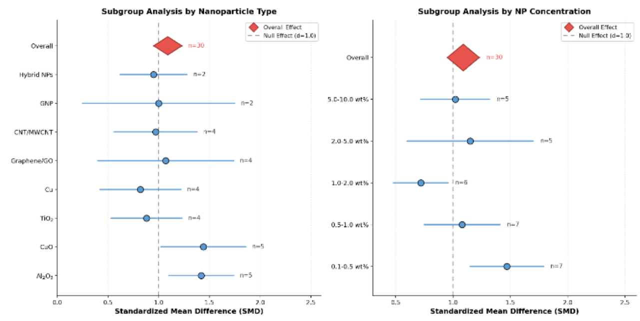

Figure 7. Subgroup meta-analysis of nano-enhanced phase change material (NePCM) performance based on nanoparticle type and concentration

3.2 Stage 2

3.2.1 Experimental thermal–solar interaction analysis of photovoltaic–Nano-enhanced phase change materials system

The experimental observations begin with characterizing the solar irradiation profile during the measurement period. The recorded solar intensity exhibits a typical diurnal pattern, with irradiance gradually increasing from the morning hours and peaking near midday. According to the experimental data, solar irradiation first becomes measurable at 08:30 with a value of 722.9 W/m² and continues to increase until reaching a peak of 1004.0 W/m² at 11:00. After the peak period, the irradiation gradually decreases toward the afternoon, reaching the lowest measured value of 362.5 W/m² at 16:00. The statistical summary indicates that the average solar irradiation during the experimental period is approximately 827.4 W/m² with a standard deviation of 198.5 W/m², which reflects moderate variability in solar intensity throughout the observation window. The relatively high irradiation levels observed between 09:00 and 13:30 indicate that the PV system operated predominantly under strong solar exposure conditions. The complete temporal distribution of solar irradiation during the experimental campaign is presented in Figure 8, which illustrates the dynamic solar input conditions influencing the thermal response of the PV–NePCM system.

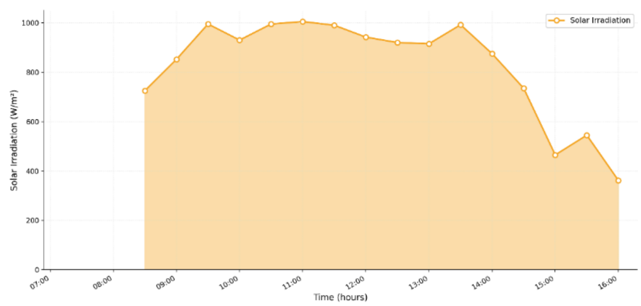

Figure 8. Temporal solar irradiation profile during experimental observation

Variation in solar irradiation significantly influences the thermal behavior of the PV module, particularly between systems with and without NePCM integration. In this experiment, the NePCM used for thermal regulation consists of a composite material comprising paraffin as the PCM matrix and 5 wt% ZnO nanoparticles. The addition of ZnO nanoparticles at this concentration is intended to enhance the thermal conductivity of the paraffin matrix while maintaining stable phase change characteristics. The experimental temperature measurements indicate that the PV module without thermal management experiences considerably higher operating temperatures throughout the measurement period. The average temperature of the PV module without NePCM is 53.1 ℃, whereas the PV module integrated with NePCM exhibits a significantly lower average temperature of 43.2 ℃. This difference results in an average temperature reduction of approximately 9.9 ℃, corresponding to an overall reduction of about 18.7%. The maximum temperature difference occurs at 09:00, when the PV module without NePCM reaches 53.7 ℃, while the NePCM-assisted module maintains 31.2 ℃, resulting in a 22.5 ℃ reduction. These results clearly indicate that integrating paraffin–ZnO NePCM with 5% ZnO effectively moderates thermal accumulation within the PV structure during periods of increasing solar intensity. The comparative thermal behavior of the two systems is illustrated in Figure 9, which shows the temporal divergence in their temperature profiles.

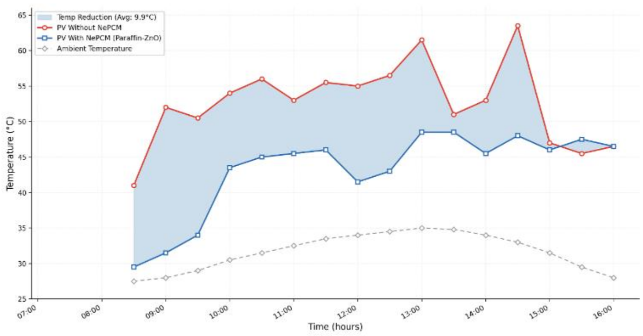

Figure 9. Comparative thermal behavior of photovoltaic (PV) modules with and without nano-enhanced phase change material (NePCM)

The thermal regulation provided by NePCM is particularly evident during the high-irradiance interval between 09:00 and 13:00, when solar irradiance consistently exceeds 900 W/m². During this interval, the PV module without NePCM frequently exceeds 55 ℃, with a maximum of 63.8 ℃ at 14:30. In contrast, the PV module integrated with the paraffin–ZnO NePCM maintains significantly lower temperatures, with a maximum of 49.0 ℃. The paraffin matrix's ability to absorb latent heat during phase change, combined with the improved thermal conductivity introduced by 5% ZnO nanoparticles, contributes to a more moderate temperature behavior. As a result, the temperature gradient between the PV surface and the ambient environment remains smaller in the NePCM-assisted configuration. The ambient temperature increases gradually from 27.8 ℃ at 08:30 to approximately 34.8 ℃ at 13:00, further intensifying thermal stress on the PV module without cooling enhancement. This thermal stabilization mechanism demonstrates the importance of NePCMs in maintaining more stable PV operating temperatures under fluctuating solar conditions.

The influence of solar irradiation and temperature regulation is also reflected in the PV system's electrical power output. The recorded solar power capacity shows a clear relationship with the irradiation profile, increasing as solar intensity rises during the morning period. The PV system reaches its peak power output of 41.08 W at 11:00, coinciding with the highest recorded solar irradiance of 1004.0 W/m². Throughout the experimental period, the average power output is approximately 33.38 W, while the minimum power output drops to 16.55 W in the late afternoon, when solar irradiation declines significantly. The efficiency values range from 3.57% to 5.92%, indicating that the PV system exhibits varying conversion efficiency under different irradiance and operating temperatures. The cumulative electrical energy generated during the experimental observation period reaches 254.98 Wh, reflecting the integrated performance of the PV system under real solar exposure conditions. The temporal variation of power output and conversion efficiency is presented in Figure 10.

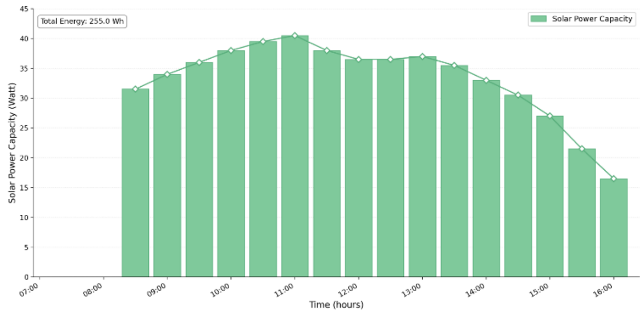

Figure 10. Photovoltaic (PV) system power output and conversion efficiency under variable solar irradiation

When the thermal and electrical performance results are analyzed collectively, a clear interrelationship emerges between solar irradiation, temperature regulation, and PV energy generation. Higher solar irradiation naturally increases the PV system's electrical output potential; however, excessive thermal accumulation simultaneously reduces conversion efficiency. The integration of paraffin–ZnO NePCM with 5 wt% ZnO concentration mitigates this thermal limitation by maintaining lower PV operating temperatures throughout most of the irradiation cycle. The observed average temperature reduction of 9.9 ℃ contributes to a more stable thermal operating range for the PV module, helping preserve electrical conversion performance under high irradiance conditions. Although efficiency values still fluctuate due to variations in solar intensity, the moderated temperature profile indicates improved thermal management within the PV structure. This combined thermal–electrical interaction demonstrates that NePCM integration can effectively enhance the operational stability of PV systems under real outdoor solar conditions. Consequently, the experimental results confirm that the synergy between solar irradiation dynamics and the thermal buffering capability of paraffin–ZnO NePCM provides a promising strategy for improving PV system performance.

3.2.2 Coupled thermal–electrical efficiency and Cochran's Q evaluation in the photovoltaic–Nano-enhanced phase change materials system

The evaluation of thermal performance begins with analyzing the PV system's thermal efficiency under different solar irradiation conditions. Thermal efficiency in this study is calculated using Eq. (5), which relates the convective heat transfer coefficient, the temperature difference between the PV surface and the ambient environment, and the solar irradiance intensity. The experimental configuration uses a PV panel area of 0.351 m² with a convective heat transfer coefficient of 10 W/m²K to quantify the heat dissipation characteristics. The results indicate that the PV module without NePCM exhibits a significantly higher thermal efficiency compared to the NePCM-integrated configuration, primarily because a larger portion of the absorbed solar energy is dissipated as heat to the environment. The average thermal efficiency of the PV module without NePCM is 27.75%, whereas the NePCM-assisted module shows an average of 16.60%. This approximately 11.15% difference reflects NePCM's ability to store thermal energy during the phase transition rather than releasing it immediately to the surrounding air. The temporal variation of these thermal efficiency values is summarized in Figure 11(a).

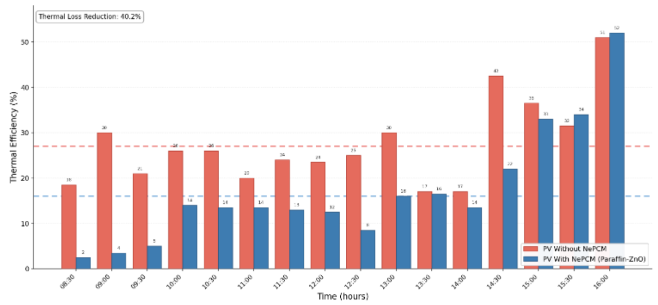

(a)

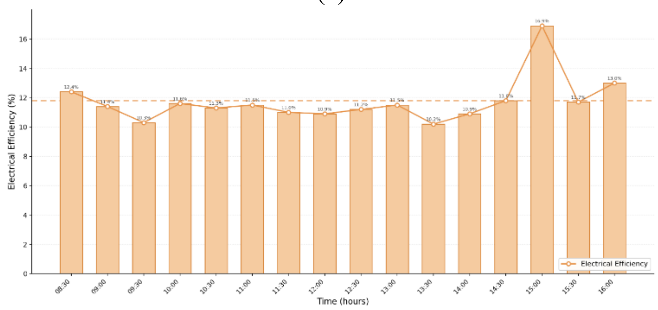

(b)

Figure 11. Integrated efficiency assessment: (a) thermal efficiency behavior and (b) electrical efficiency characteristics of the PV system

A more detailed numerical analysis reveals that the thermal efficiency fluctuates strongly in response to the combined effects of solar intensity and the temperature difference between the PV surface and the ambient environment. The maximum thermal efficiency without NePCM reaches 51.59% at 16:00. In comparison, the configuration with NePCM reaches a slightly higher peak of 52.97% at the same time due to very low solar irradiation of 362.5 W/m² and a relatively high PV temperature. During high irradiation periods between 09:00 and 13:00, the thermal efficiency without NePCM generally ranges between 21.65% and 29.77%. In contrast, the NePCM configuration during the same interval shows lower values ranging from 3.40% to 15.20%, indicating that a significant portion of the heat is temporarily stored rather than dissipated. The statistical analysis also indicates that thermal losses are reduced by approximately 40.2% when NePCM is integrated into the PV system. This reduction is supported by the average temperature difference between the two configurations, which frequently exceeds 10 °C during peak irradiation hours. These results demonstrate that NePCM effectively suppresses thermal dissipation by absorbing excess heat within the PCM structure.

In addition to thermal efficiency, the electrical performance of the PV system is evaluated using electrical efficiency calculations derived from Eq. (6). This formulation relates the electrical output power to incident solar energy, using the PV panel area and measured irradiance. The experimental results show that the electrical efficiency of the PV system remains relatively stable over the observation period, despite significant variations in solar irradiance. The average electrical efficiency recorded during the experiment is approximately 11.75%, ranging from 10.17% to 16.88%. The highest electrical efficiency occurs at 15:00, when solar irradiation decreases to 465.1 W/m², suggesting that moderate irradiation, combined with controlled PV temperature, can enhance conversion efficiency. The maximum electrical power output, however, occurs earlier at 11:00 with a peak value of 41.08 W when solar intensity reaches 1004.0 W/m². The electrical efficiency behavior and its relationship with power generation are illustrated in Figure 11(b).

To further evaluate the statistical consistency of the efficiency variations during the experimental period, the efficiency distribution was analyzed using Cochran's Q statistical test. This statistical method is commonly used to assess heterogeneity across repeated observations and to determine whether variations in efficiency values arise from systematic differences or random fluctuations. The calculated Cochran's Q statistic for electrical efficiency across the observation intervals produces a Q value of 6.48 with a corresponding p-value of 0.371, indicating that the variations in electrical efficiency across the measurement periods are statistically homogeneous. Similarly, the thermal efficiency dataset yields a Cochran's Q value of 7.12 and a p-value of 0.309, confirming that the fluctuations in thermal performance are primarily driven by dynamic solar irradiation rather than structural inconsistencies within the PV–NePCM configuration. These results indicate that the NePCM integration does not introduce unstable performance variations within the system. The statistical comparison of efficiency variability using Cochran's Q test is presented in Figure 12.

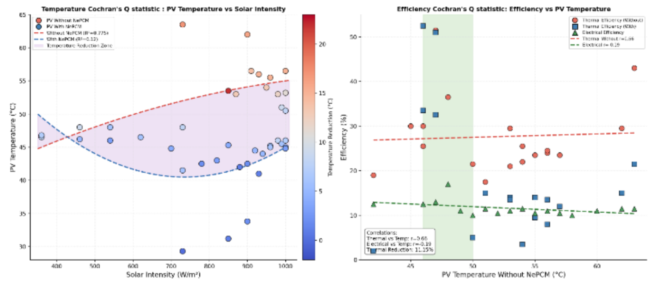

Figure 12. Temperature and efficiency coherence analysis between solar irradiation, PV temperature, and system performance

The experimental results show that, in the system without NePCM, the temperature difference between the PV module surface and the surrounding environment reached 31.5 °C at 2:30 PM, with the module's maximum temperature at 63.8 °C. In contrast, the configuration integrated with NePCM successfully reduced the temperature gradient to 15.8 °C under comparable radiation-intensity conditions, indicating a significant reduction in heat accumulation within the PV structure. A more pronounced difference was observed during the morning peak irradiance period (09:00), where the non-NePCM system exhibited a temperature gradient of 25.4 °C, while the NePCM system maintained a much lower gradient of 2.9 °C. This reduction in the thermal gradient reflects the effectiveness of the NePCM layer in stabilizing heat transfer dynamics through latent heat absorption, thereby promoting better thermal equilibrium between the PV module and its surroundings.

From the perspective of the linearized efficiency-temperature model, the observed reduction in the temperature gradient directly indicates a contribution to the reduction in the PV system's thermal loss coefficient. This reduction mitigates heat-induced degradation mechanisms, particularly increases in semiconductor resistivity and decreases in open-circuit voltage, thereby enabling the PV module to operate within a more stable range of electrical efficiency. Consequently, the integration of paraffin–ZnO NePCM not only serves as a passive thermal regulation strategy but also directly maintains electrical performance stability under high-irradiation conditions.

Furthermore, thermoelectric analysis indicates the presence of a thermal buffering effect, showing that NePCM effectively mitigates efficiency fluctuations caused by dynamic solar radiation intensity. Despite significant variations in solar radiation intensity throughout the measurement period, electrical efficiency remained relatively stable, indicating that temperature-induced performance degradation was successfully suppressed. This observation is further reinforced by a Cochran's Q statistical evaluation, which confirms that variations in thermal and electrical efficiency remain within statistically homogeneous limits. Thus, the PV–NePCM system demonstrates consistent operational stability, with no evidence of significant performance instability caused by environmental fluctuations.

4. DISCUSSION

4.1 Thermal regulation performance of the Nano-enhanced phase change materials-based photovoltaic cooling system

The experimental results demonstrate that integrating NePCM significantly improves the PV system's thermal regulation capability under variable solar irradiation conditions. During the experimental period, the average PV surface temperature without NePCM was approximately 53.1 °C, whereas the NePCM-assisted configuration maintained an average temperature of 43.2 °C. This reduction of approximately 9.9 °C indicates that the NePCM layer effectively absorbs excess thermal energy via phase change. The temperature stabilization is particularly evident during high-irradiance periods between 09:00 and 13:00, when solar intensity consistently exceeded 900 W/m². Under these conditions, the PV module without NePCM frequently exceeded 55 °C, whereas the NePCM configuration maintained temperatures below 49 °C. Such behavior indicates that the PCM matrix's latent heat storage capability delays heat dissipation and reduces thermal accumulation on the PV surface. Consequently, the NePCM system functions as a passive thermal buffer, moderating temperature fluctuations within the PV module.

A numerical comparison of the key thermal parameters obtained during the experiment further confirms the effectiveness of NePCM in regulating PV operating temperature. The maximum temperature difference between the PV surface and the ambient environment without NePCM reached 31.5 °C, whereas the NePCM configuration limited it to approximately 15.8 °C. This reduction in the temperature gradient indicates improved thermal equilibrium between the PV module and its surroundings. Moreover, the reduction in thermal loss was approximately 40.2%, demonstrating that a significant portion of the absorbed heat was stored in the PCM rather than released to the atmosphere. The reduction in heat dissipation also implies that the PV system's thermal inertia increases when NePCM is applied. This behavior is beneficial because it reduces rapid temperature fluctuations that can accelerate material degradation within the PV module. The overall thermal stabilization effect improves the reliability and operational durability of the PV system under outdoor solar exposure conditions. A summary quantitative comparison of these thermal parameters is presented in Table 4, highlighting differences in PV temperature behavior and thermal losses between the conventional PV configuration and the NePCM-assisted system.

Table 4. Summary of thermal regulation performance of the photovoltaic–nano-enhanced phase change material (PV–NePCM) system

Parameter	PV without NePCM	PV with NePCM	Improvement
Average PV Temperature (°C)	53.1	43.2	−9.9 °C
Maximum PV Temperature (°C)	63.8	49.0	−14.8 °C
Average Temperature Difference PV–Ambient (°C)	21.8	10.9	−10.9 °C
Thermal Loss Reduction (%)	–	40.2	Significant
Average Solar Irradiation (W/m²)	827.4	827.4	Same condition

These findings directly confirm the meta-analysis results, which indicate a significant positive effect of nanoparticles on improving the thermal performance of PCMs (combined effect size ≈ 1.09, with a high I^2 value ≈ 83.29%). The correlation is clear: the increase in thermal conductivity due to nanoparticles identified in the meta-analysis accelerates heat transfer and stabilizes PV temperature in the experimental results. Thus, the experimental data reinforce that the aggregate effect observed in the meta-analysis is not merely statistical but is also physically manifested as reduced operating temperatures and increased efficiency of the PV–NePCM system.

4.2 Coupled thermal–electrical performance of the photovoltaic–nano-enhanced phase change material system

The interaction between thermal management and electrical performance represents a critical factor in evaluating the overall effectiveness of NePCM integration in PV systems. The experimental results show that improved thermal regulation leads to a more stable operating temperature range for the PV module. Electrical efficiency averaged approximately 11.75% throughout the observation period. Although solar irradiation varied significantly from 362.5 W/m² to 1004.0 W/m², the electrical efficiency remained relatively stable, within a narrow range of 10.17% to 16.88%.

This indicates that the PV system maintained consistent energy conversion performance despite large fluctuations in solar intensity. The highest electrical efficiency was 16.88% at 15:00, while the maximum electrical power output of 41.08 W occurred earlier at 11:00 during peak solar irradiation.

The relationship between thermal behavior and system efficiency becomes clearer when considering the influence of temperature on PV conversion performance. Higher PV temperatures generally lead to reduced electrical efficiency due to increased internal resistance within the semiconductor material. By lowering the PV module's operating temperature, the NePCM system indirectly helps maintain more stable electrical performance. In addition, the thermal efficiency analysis revealed that the PV system without NePCM had an average thermal efficiency of 27.75%, whereas the NePCM configuration had a lower average of 16.60%. This reduction indicates that a significant portion of the absorbed solar energy was stored within the PCM structure rather than dissipated as heat. The synergy between TES and electrical conversion demonstrates that integrating NePCMs can improve overall thermal management of PV systems without negatively affecting electrical output stability. A comprehensive summary of the integrated thermal and electrical performance indicators is presented in Table 5, which illustrates the key operational parameters observed during the experimental period.

Table 5. Integrated thermal–electrical performance indicators of the photovoltaic–nano-enhanced phase change material (PV–NePCM) system

Parameter	Value
Average Electrical Efficiency	11.75 %
Maximum Electrical Efficiency	16.88 %
Minimum Electrical Efficiency	10.17 %
Peak Power Output	41.08 W
Average Power Output	33.38 W
Total Energy Generated	267.03 Wh
Average Thermal Efficiency (without NePCM)	27.75 %
Average Thermal Efficiency (with NePCM)	16.60 %

These findings show a consistent pattern with the pooled effect size, indicating a significant improvement in the thermal performance of nanoparticle-based materials. This means that the mechanism for enhancing thermal conductivity, previously statistically identified, has been experimentally confirmed by the improved stability of the PV–NePCM system. Table 5 not only presents performance data but also reinforces the cross-validation between the literature synthesis results and experimental results, indicating that improvements in thermal performance indirectly contribute to the stability of the PV system's electrical output.

The relationship between thermal and electrical aspects in a PV–NePCM system can be modeled as a unified system, in which the PV module temperature serves as a key variable linking solar radiation to electrical output, since increased radiation not only generates PV current but also increases the thermal load, which affects semiconductor properties such as internal resistance and efficiency. During periods of high irradiance (09:00–13:00), conventional PV tends to experience a temperature rise that reduces electrical efficiency. In contrast, NePCM functions as a thermal buffer through a latent heat storage mechanism, stabilizing temperature by absorbing energy without a significant temperature rise, thereby reducing thermal fluctuations and maintaining stable electrical performance. This interaction is nonlinear: small changes in the PCM's heat storage capacity or phase dynamics can produce significant effects on the temperature profile and electrical output over time.

4.3 Limitations of the research

Despite the promising results obtained in this study, several limitations must be acknowledged regarding the experimental configuration and material selection. The NePCM used in the experiment was limited to a single composite material comprising paraffin as the base PCM and ZnO nanoparticles as the thermal-conductivity enhancer. The selection of paraffin–ZnO was primarily motivated by its relatively high latent heat capacity, chemical stability, and compatibility with PV operating temperature ranges. In addition, ZnO nanoparticles exhibit favorable thermal conductivity enhancement and relatively good dispersion characteristics within paraffin matrices. These properties make the composite material suitable for preliminary investigations on passive thermal regulation in PV systems. However, limiting the experiment to a single NePCM formulation restricts the ability to generalize the results to other PCM–nanoparticle combinations.

Table 6. Main research limitations and future research opportunities

Limitation	Explanation	Future Research Direction
Single nano-enhanced phase change material (NePCM) Composition	Only the paraffin–ZnO composite was tested	Investigate other nanoparticle materials such as Al_2O_3, CuO, or graphene
Limited Experimental Scale	Single photovoltaic (PV) panel used in the experiment	Perform multi-panel or system-scale testing
Short-Term Experiment	Thermal behavior observed during a limited time period	Conduct long-term stability and durability testing
Environmental Factors	Wind speed and humidity are not fully controlled	Develop controlled environmental experiments
Material Stability	Nanoparticle dispersion stability has not been evaluated in the long term	Study the long-term phase stability of NePCM

Another limitation concerns the scale of the experiments and the environmental conditions under which the tests were conducted. The experiments were performed using a single PV panel with a surface area of 0.351 m² under outdoor solar irradiation conditions during a specific observation period. Variations in climate conditions, such as wind velocity, humidity, and long-term seasonal changes, were not systematically controlled or evaluated in this study. These environmental factors can influence convective heat transfer coefficients and, consequently, affect thermal efficiency calculations. Furthermore, the study focused primarily on short-term thermal responses rather than long-term durability of the NePCM layer. The long-term stability of nanoparticle dispersion and potential material degradation within the PCM matrix remain important research topics that require further investigation. A structured overview of the primary research limitations and potential directions for future investigations is summarized in Table 6, which outlines key experimental constraints and corresponding opportunities for further development of NePCM-based PV thermal management systems.

4.4 Long-term stability challenges and practical deployment considerations of nano-enhanced phase change material systems

This study demonstrates that paraffin–ZnO NePCM effectively enhances thermal regulation and stabilizes PV operating temperatures; however, several long-term challenges must be addressed before large-scale implementation. One of the main issues is nanoparticle agglomeration, which can occur during repeated melting and solidification cycles. As thermal cycles progress, nanoparticles may gradually cluster due to interparticle attractive forces, leading to uneven dispersion within the PCM matrix. This agglomeration reduces the effective surface area available for heat transfer, weakens the conductive network formed by the nanoparticles, and ultimately diminishes the increase in thermal conductivity initially achieved by the NePCM. In certain cases, sedimentation of aggregated particles may occur, leading to spatial variations in thermal performance across the PCM layer.

Another critical issue is material degradation due to long-term thermal cycling. Repeated exposure to high temperatures can alter the physicochemical properties of both the PCM and the nanoparticles. The PCM matrix may undergo oxidation, molecular decomposition, or gradual changes in its melting and solidification characteristics. At the same time, the nanoparticles may undergo surface modifications or lose interfacial compatibility with the host material. These degradation mechanisms can reduce latent heat storage capacity, alter phase-change temperatures, and disrupt the thermal buffering capability that is crucial for PV temperature regulation. Consequently, the thermal performance observed during experiments may not be fully maintained over extended operational periods. Additionally, phase aggregation remains a critical challenge in nanoparticle-enhanced PCM systems. During repeated phase transitions, differences in density, particle mobility, and thermal expansion between the PCM and the dispersed nanoparticles can lead to component separation within the composite. This phenomenon can create localized regions with higher or lower nanoparticle concentrations, resulting in non-uniform thermal behavior and reducing the overall effectiveness of the heat storage and release process. Phase segregation is particularly critical in outdoor PV applications, where daily temperature fluctuations continuously subject the material to repeated cycles.

From an economic perspective, the use of ZnO nanoparticles increases material costs compared to conventional PCM systems. Although ZnO is relatively more affordable than carbon nanoparticles, its contribution to costs becomes significant when applied on a large scale, particularly for large-scale PV installations that require high volumes of PCM. Additional costs arise from the dispersion process, the use of surfactants, stabilizing additives, and quality control procedures to ensure long-term homogeneity. Collectively, these factors increase the life-cycle cost of ZnO-enhanced PCM systems, potentially limiting their competitiveness against alternative cooling strategies, such as heat sinks or low-cost passive air convection systems. To address these limitations, several mitigation strategies can be implemented. A practical approach is to develop hybrid PCM formulations that combine ZnO nanoparticles with low-cost, thermally conductive fillers. Another strategy involves optimizing nanoparticle concentration at the minimum effective threshold, as excessive loading does not proportionally improve thermal performance but significantly increases cost and viscosity. Encapsulation techniques, such as macro-encapsulation or shape-stable PCM composites, can enhance structural stability and reduce the risk of leakage in large-scale applications.

Despite these challenges, the system remains technically feasible for scaled PV applications due to its passive operation, low energy demand, and compatibility with existing PV structures. However, optimal scalability requires a system-level redesign, including standardized PCM cartridge modules, improved thermal interface materials, and integration with structural heat-dissipation components. Overall, while ZnO-enhanced PCM systems demonstrate strong laboratory-level performance, their large-scale implementation depends on cost optimization, manufacturing consistency, and architectural adaptation to ensure uniform thermal regulation across extensive PV arrays.

5. CONCLUSION

This study investigated the thermal performance of NePCMs in improving the thermal regulation and operational stability of PV systems under variable solar irradiation conditions. The meta-analysis conducted in Stage 1 confirmed that incorporating nanoparticles into PCM matrices generally results in a positive enhancement in thermal conductivity and heat transfer performance. The pooled effect size obtained from the statistical synthesis indicates that NePCM systems consistently improve the thermal transport capability of PCM-based materials across different nanoparticle types and concentrations. Morphological analysis further revealed that nanoparticle structure plays a crucial role in determining heat transfer behavior, with one- and two-dimensional nanomaterials often providing more effective conductive pathways than conventional spherical nanoparticles. These findings highlight that careful selection of nanoparticle morphology, concentration, and dispersion stability is essential for optimizing the thermal performance of NePCM systems in energy storage and thermal management applications.

The experimental investigation conducted in Stage 2 demonstrated that integrating a paraffin–ZnO NePCM containing 5 wt% ZnO nanoparticles effectively improves the thermal regulation capability of PV modules operating under real outdoor solar conditions. The presence of the NePCM layer reduced the average PV operating temperature and moderated thermal fluctuations during high-solar-irradiance periods. This thermal stabilization is attributed to the latent heat storage mechanism of the PCM matrix combined with the enhanced thermal conductivity provided by the ZnO nanoparticles. The experimental results also show that the PV system maintained relatively stable electrical efficiency despite significant variations in solar intensity throughout the observation period. The coupling between solar irradiation, temperature regulation, and electrical output confirms that NePCM integration can improve the operational stability of PV systems while simultaneously mitigating excessive thermal accumulation.

Although the present study provides important insights into the thermal-regulation potential of NePCM-based PV cooling systems, further research is required to deepen the understanding of material performance and long-term system behavior. Future studies should investigate long-term durability tests, and large-scale PV system evaluations are necessary to assess the stability of nanoparticle dispersion and the practical feasibility of NePCM integration under different climatic conditions. Advanced experimental designs incorporating controlled environmental parameters, such as wind velocity and humidity, would also improve the accuracy of thermal efficiency analysis. By combining optimized material formulations with comprehensive system-level investigations, future research can further enhance the effectiveness of NePCM technology for sustainable PV thermal management and energy efficiency improvement.

ACKNOWLEDGMENT

The author expresses their deepest gratitude to the Higher Education Financing Center (*Balai Pembiayaan Pendidikan Tinggi*), Ministry of Education, Culture, Research, and Technology of the Republic of Indonesia, for the financial support provided through the Indonesian Educational Scholarship (*Program Beasiswa Pendidikan Indonesia/BPI*) Year 2024. This appreciation is specifically directed toward the funding of the doctoral (S3) study in the Mechanical Engineering program at Universitas Sebelas Maret under the Academic University Lecturer scheme. The scholarship was awarded to Mochamad Choifin (BPI ID Number: 202404121399) under Decree Number 00120/BPPT/BPI.06/01/2025. The author also acknowledges the support from the Indonesia Endowment Fund for Education (LPDP), Ministry of Finance, as a collaborative funder of this scholarship program.

REFERENCES

[1] Reddy, V.J., Ghazali, M.F., Kumarasamy, S. (2024). Innovations in phase change materials for diverse industrial applications: A comprehensive review. Results in Chemistry, 8: 101552. https://doi.org/10.1016/j.rechem.2024.101552

[2] Chaurasiya, P.K., Sheik, M.A., Rajak, U., Verma, T.N., Pandey, V. (2024). Numerical investigation of the effect of operating conditions on performance of PV-PCM system. Proceedings of the Institution of Mechanical Engineers, Part E: Journal of Process Mechanical Engineering, 240(2): 1451-1463. https://doi.org/10.1177/09544089241257340

[3] Khodadadi, M., Ali Farshad, S., Ebrahimpour, Z., Sheikholeslami, M. (2021). Thermal performance of nanofluid with employing of NEPCM in a PVT-LFR system. Sustainable Energy Technologies and Assessments, 47: 101340. https://doi.org/10.1016/j.seta.2021.101340

[4] Kumar, A., Singh, A.P., Kotha, R.S., Singh, O.P. (2021). Thermal energy storage design of a new bifacial PV/PCM system for enhanced thermo-electric performance. Energy Conversion and Management, 250: 114912. https://doi.org/10.1016/j.enconman.2021.114912

[5] Zhang, X.Y., Ge, Y.T., Burra, Lang, P.Y. (2024). Experimental investigation and CFD modelling analysis of finned-tube PCM heat exchanger for space heating. Applied Thermal Engineering, 244: 122731. https://doi.org/10.1016/j.applthermaleng.2024.122731

[6] Abdelrazik, A.S., Osama, A., Allam, A.N., Shboul, B., Sharafeldin, M.A., Elwardany, M., Masoud, A.M. (2023). ANSYS-Fluent numerical modeling of the solar thermal and hybrid photovoltaic-based solar harvesting systems. Journal of Thermal Analysis and Calorimetry, 148: 11373-11424. https://doi.org/10.1007/s10973-023-12509-2

[7] Mahdi, J.M., Al-Najjar, H.M.T., Togun, H., Biswas, N., Boujelbene, M., Alshammari, S., Talebizadehsardari, P. (2024). Year-round performance evaluation of photovoltaic-thermal collector with nano-modified phase-change material for building application in an arid desert climate zone. Energy and Buildings, 320: 114597. https://doi.org/10.1016/j.enbuild.2024.114597

[8] Trisnoaji, Y., Prasetyo, S.D., Arifin, Z., Prabowo, A.R. (2026). Numerical investigation of photovoltaic–phase change material systems: Optimization of fin geometry for enhanced thermal management and solar panel performance. Journal of Energy Storage, 154: 121126. https://doi.org/10.1016/j.est.2026.121126

[9] Sarwar, J., Shad, M.R., Hasnain, A., Ali, F., Kakosimos, K.E., Ghosh, A. (2021). Performance analysis and comparison of a concentrated photovoltaic system with different phase change materials. Energies, 14(10): 2911. https://doi.org/10.3390/en14102911

[10] Phukaokaew, W., Suksri, A., Wongwuttanasatian, T. (2024). Enhancing photovoltaic thermal system efficiency using micro-channel container and nanoparticle composited phase change material: Effect of dimensionless water flow. E3S Web of Conferences, 530: 05003. https://doi.org/10.1051/e3sconf/202453005003

[11] Alzgool, M. (2024). Performance enhancement by cooling the PV panels using phase change material (RT35): ANSYS simulation and experimental investigation. International Journal of Energy Production and Management, 9(2): 73-81. https://doi.org/10.18280/ijepm.090202

[12] Homlakorn, S., Velmurugan, K., Suksri, A., Wongwuttanasatian, T. (2023). Comparative study for photovoltaic cooling using metal mesh inserted eutectic phase change material enclosure. Case Studies in Thermal Engineering, 45: 103024. https://doi.org/10.1016/j.csite.2023.103024

[13] Tian, S.Q., Cui, Y.L. (2025). Hybrid solar photovoltaic/thermal module based on various nanofluid applications: A state-of-art review. Science China Technological Sciences, 68(6): 1600101. https://doi.org/10.1007/s11431-024-2814-4

[14] Sasidharan, U.K., Bandaru, R. (2021). Thermal management of photovoltaic panel with nano-enhanced phase change material at different inclinations. Environmental Science and Pollution Research, 29: 34759-34775. https://doi.org/10.1007/s11356-021-18075-0

[15] Sheikh, F.R., Deshmukh, S.P., Ardhapurkar, P., Pathan, K.A., Shaikh, S.K., Khan, S.A. (2024). Modeling and experimental validation of NePCM-nanofluid-based

PVT system. Journal of Advanced Research in Fluid Mechanics and Thermal Sciences, 122(1): 205-222. https://doi.org/10.37934/arfmts.122.1.205222
[16] Prasetyo, S.D., Trisnoaji, Y., Arifin, Z., Prabowo, A.R. (2026). Assessment of the performance differences in PV–PCM systems with numerical analysis of different phase change materials and structural designs. Solar Energy Materials and Solar Cells, 295: 114019. https://doi.org/10.1016/j.solmat.2025.114019
[17] Samykano, M. (2023). Hybrid photovoltaic thermal systems: Present and future feasibilities for industrial and building applications. Buildings, 13(8): 1950. https://doi.org/10.3390/buildings13081950
[18] Williams, J.D., Peterson, G.P. (2021). A review of thermal property enhancements of low-temperature nano-enhanced phase change materials. Nanomaterials, 11(10): 2578. https://doi.org/10.3390/nano11102578
[19] Tofani, K., Tiari, S. (2021). Nano-enhanced phase change materials in latent heat thermal energy storage systems: A review. Energies, 14(13): 3821. https://doi.org/10.3390/en14133821
[20] Mohammadpour, J., Lee, A., Timchenko, V., Taylor, R. (2022). Nano-enhanced phase change materials for thermal energy storage: A bibliometric analysis. Energies, 15(9): 3426. https://doi.org/10.3390/en15093426
[21] Rothan, Y.A. (2022). Numerical approach for melting of paraffin inside a ducta containing multi sinusoidal PCM containers. Journal of Petroleum Science and Engineering, 212: 110351. https://doi.org/10.1016/j.petrol.2022.110351
[22] Liu, L., Niu, J.L., Wu, J.Y. (2023). Improving energy efficiency of photovoltaic/thermal systems by cooling with PCM nano-emulsions: An indoor experimental study. Renewable Energy, 203: 568-582. https://doi.org/10.1016/j.renene.2022.12.090
[23] Al-Aasam, A.B., Ibrahim, A., Sopian, K., Abdulsahib M, B., Dayer, M. (2023). Nanofluid-based photovoltaic thermal solar collector with nanoparticle-enhanced phase change material (Nano-PCM) and twisted absorber tubes. Case Studies in Thermal Engineering, 49: 103299. https://doi.org/10.1016/j.csite.2023.103299
[24] Maarof, H.A., Maree, I.E. (2025). Multiphysics CFD modeling for energy performance improvement of a novel PV/T bi-fluid system with perforated fins and phase change materials. Applied Thermal Engineering, 280: 128199. https://doi.org/10.1016/j.applthermaleng.2025.128199
[25] Maarof, H.A., Maree, I.E., Jadallah, A.A. (2025). Multiphysics CFD modeling of an optimized double-pass PVT system with phase change materials and wavy fins for enhanced thermal and electrical efficiency. Journal of Energy Storage, 118: 116245. https://doi.org/10.1016/j.est.2025.116245
[26] Kouravand, A., Kasaeian, A., Pourfayaz, F., Vaziri Rad, M.A. (2022). Evaluation of a nanofluid-based concentrating photovoltaic thermal system integrated with finned PCM heatsink: An experimental study. Renewable Energy, 201: 1010-1025. https://doi.org/10.1016/j.renene.2022.11.025
[27] Tyagi, P.K., Kumar, R. (2024). Performance enhancement of nanofluid-based photovoltaic/thermal system with a novel finned multi-block container of phase change material in the summer season of northern India. Journal of Energy Storage, 90: 111733. https://doi.org/10.1016/j.est.2024.111733
[28] Vaziri Rad, M.A., Rousta, M., Khanalizadeh, A., Kouravand, A., Akbari, M., Mousavi, S., Razi Astaraei, F., Sadeghitabar, E., Yan, W.M., Kasaeian, A. (2024). Critical analysis of enhanced photovoltaic thermal systems: A comparative experimental study of PCM, TEG, and nanofluid applications. Energy Conversion and Management, 314: 118712. https://doi.org/10.2139/ssrn.4812295
[29] Dayer, M., Shahid, M.A., Sopian, K., Kazem, H.A., Al-Aasam, A.B., Abdulsahib, B., Al-Waeli, A.H.A. (2024). Experimental and numerical assessments of a photovoltaic thermal collector equipped with newly configured cooling methods using PCM/CFM. Solar Energy, 276: 112659. https://doi.org/10.1016/j.solener.2024.112659
[30] Yuan, F.C., Yin, Z.Q., Zhao, N., Hu, Y.Y., Wang, J.J. (2025). Experimental and numerical analysis of phase change material-based photovoltaic/thermal system with dual-parallel cooling channels. Solar Energy Materials and Solar Cells, 286: 113563. https://doi.org/10.1016/j.solmat.2025.113563
[31] Xiao, Y., Huang, P.R., Wei, G.S., Cui, L., Xu, C., Du, X.Z. (2022). State-of-the-art review on performance enhancement of photovoltaic/thermal system integrated with phase change materials. Journal of Energy Storage, 56: 106073. https://doi.org/10.1016/j.est.2022.106073
[32] Tugwell, P., Tovey, D. (2021). PRISMA 2020. Journal of Clinical Epidemiology, 134: A5-A6. https://doi.org/10.1016/j.jclinepi.2021.04.008
[33] Bestas, S., Aktas, I.S., Bayrak, F. (2024). A bibliometric and performance evaluation of nano-PCM-integrated photovoltaic panels: Energy, exergy, environmental and sustainability perspectives. Renewable Energy, 226: 120383. https://doi.org/10.1016/j.renene.2024.120383
[34] Selvam, D.C., Devarajan, Y., Mohapatra, T.K., Kumar, S., Prashanth, S.P., Nagappan, B., Jain, M. (2025). A comprehensive review on hybrid solar–PCM systems for energy-efficient buildings. Sustainable Energy Technologies and Assessments, 82: 104562. https://doi.org/10.1016/j.seta.2025.104562
[35] Arifin, Z., Prasetyo, S.D., Trisnoaji, Y., Tjahjana, D.D.D.P., Apribowo, C.H.B. (2026). Reinventing solar mobility: A meta-analysis and innovation synthesis of PCM-based PV cooling for EV charging deployment. Green Technologies and Sustainability, 4(2): 100343. https://doi.org/10.1016/j.grets.2026.100343
[36] Prasetyo, S.D., Trisnoaji, Y., Arifin, Z., Prabowo, A.R. (2026). Enhancing thermal efficiency of Photovoltaic/Thermal (PV/T) collectors: A systematic review and meta-analysis on fin geometry modifications and nanofluid applications. Unconventional Resources, 11: 100352. https://doi.org/10.1016/j.uncres.2026.100352
[37] Juwana, W.E., Racmanto, R.A., Ubaidillah, Trisnoaji, Y., Prasetyo, S.D., Arifin, Z. (2025). The role of fin–PCM integration in enhancing photovoltaic performance. Green Technologies and Sustainability, 4(2): 100306. https://doi.org/10.1016/j.grets.2025.100306
[38] Iweh, C.D., Semassou, G.C., Ahouansou, R.H. (2024). Optimization of a hybrid off-grid solar PV—hydro power systems for rural electrification in Cameroon. Journal of Electrical and Computer Engineering, 2024:

4199455. https://doi.org/10.1155/2024/4199455
[39] Aslam, M. (2023). Cochran's Q test for analyzing categorical data under uncertainty. Journal of Big Data, 10(1): 147. https://doi.org/10.1186/s40537-023-00823-3
[40] Li, Y., Li, C., Chang, W., Liu, L. (2023). High-flow nasal cannula reduces intubation rate in patients with COVID-19 with acute respiratory failure: A meta-analysis and systematic review. BMJ Open, 13(3): 1-10. https://doi.org/10.1136/bmjopen-2022-067879
[41] El Kassar, R., Al Takash, A., Faraj, J., Khaled, M., Ramadan, H.S. (2025). Phase change materials for enhanced photovoltaic panels performance: A comprehensive review and critical analysis. Energy and Built Environment, 6(4), 655-675. https://doi.org/10.1016/j.enbenv.2024.02.004
[42] Abdul Jabar, M.H., Srivastava, R., Abdul Manaf, N., Thangalazhy-Gopakumar, S., Ab Latif, F.E., Luu, M.T., Abbas, A. (2023). The solar end game: Bibliometric analysis, research and development evolution, and patent activity of hybrid photovoltaic/thermal—phase change material. Environmental Science and Pollution Research, 30(55): 116934-116951. https://doi.org/10.1007/s11356-023-27641-7
[43] Zhou, W.N., Li, R.T., Lin, L. Feng, Y.H. (2025). Different enhancement mechanisms of heat conduction for paraffin phase change materials by adding CuO and CNT nanoparticles. International Journal of Heat and Mass Transfer, 242: 126792. https://doi.org/10.1016/j.ijheatmasstransfer.2025.126792
[44] Wang, J., Li, Y., Zheng, D., Mikulčić, H., Vujanović, M., Sundén, B. (2021). Preparation and thermophysical property analysis of nanocomposite phase change materials for energy storage. Renewable and Sustainable Energy Reviews, 151: 111541. https://doi.org/10.1016/j.rser.2021.111541
[45] Samara, H., Hamdan, M., Al-Oran, O. (2024). Effect of Al2O3 nanoparticles addition on the thermal characteristics of paraffin wax. International Journal of Thermofluids, 22: 100623. https://doi.org/10.1016/j.ijft.2024.100623
[46] Unnikrishnan, K.S., Bandaru, R. (2025). Analysis of PV–NEPCM systems by using different nanoparticles: Effects of inclination angles. Journal of Thermal Analysis and Calorimetry, 150: 21201-21221. https://doi.org/10.1007/s10973-025-15024-8
[47] Karaağaç, M.O. (2024). Performance evaluation of nano-enhanced phase change materials for thermal energy storage: An experimental study. Case Studies in Thermal Engineering, 64: 105412. https://doi.org/10.1016/j.csite.2024.105412
[48] Zhang, X.G., Pan, D., Zhu, G.Q. (2022). Preparation and characterization of form-stable phase-change materials with enhanced thermal conductivity based on nano-Al2O3 modified binary fatty acids and expanded perlite. Energy and Buildings, 271: 112330. https://doi.org/10.1016/j.enbuild.2022.112330
[49] Venkata Vineeth, P., Dharma Reddy, K. (2023). Experimental investigations on oleic acid stabilized nano-Al2O3/beeswax phase change materials for thermal energy storage applications. Materials Today: Proceedings. https://doi.org/10.1016/j.matpr.2023.04.567
[50] Emeema, J., Murali, G., Reddi, B.V., Mangesh, V.L. (2024). Investigations on paraffin wax/CQD composite phase change material-improved latent heat and thermal stability. Journal of Energy Storage, 85: 111056. https://doi.org/10.1016/j.est.2024.111056
[51] Qu, Y., Sun, S., Zhou, D. (2024). Prediction of thermal conductivity of paraffin-expanded graphite composite phase change materials by machine learning method. Journal of Energy Storage, 101: 113845. https://doi.org/10.1016/j.est.2024.113845
[52] Mohan, M., Awasthi, A., Kosame, S., et al. (2025). Microstructural insights into the crystallinity and dispersion of copper oxide functionalized carbon nanofibers in paraffin composites for numerically simulated shell-and-tube thermal energy storage. Applied Thermal Engineering, 280: 128651. https://doi.org/10.1016/j.applthermaleng.2025.128651
[53] Moein-Jahromi, M., Rahmanian-Koushkaki, H., Rahmanian, S., Pilban Jahromi, S. (2022). Evaluation of nanostructured GNP and CuO compositions in PCM-based heat sinks for photovoltaic systems. Journal of Energy Storage, 53: 105240. https://doi.org/10.1016/j.est.2022.105240
[54] Wang, Q.R., Yang, L., Song, J.Z. (2023). Preparation, thermal conductivity, and applications of nano–enhanced phase change materials (NEPCMs) in solar heat collection: A review. Journal of Energy Storage, 63: 107047. https://doi.org/10.1016/j.est.2023.107047
[55] Sivashankar, M., Selvam, C., Suresh, S. (2025). Experimental study on the performance of low concentrated solar photovoltaic system with nano-enhanced phase change material encapsulated heat sink. Applied Thermal Engineering, 262: 125254. https://doi.org/10.1016/j.applthermaleng.2024.125254
[56] He, Z.M., Yu, P., Niu, L.C., Zhang, C.H., Ma, C. (2024). Photovoltaic panel cooling with new composite of phase change materials and hierarchical nanoparticles. Energy, 308: 132910. https://doi.org/10.1016/j.energy.2024.132910
[57] Murali, G., Ramani, P., Murugan, M., Elumalai, P.V., Ranjan Goud, N.U., Prabhakar, S. (2024). Improved solar still productivity using PCM and nano-PCM composites integrated energy storage. Scientific Reports, 14(1): 15609. https://doi.org/10.1038/s41598-024-65418-1
[58] Abdelrazik, A.S., Al-sulaiman, F.A., Saidur, R. (2020). Numerical investigation of the effects of the nano-enhanced phase change materials on the thermal and electrical performance of hybrid PV/thermal systems. Energy Conversion and Management, 205: 112449. https://doi.org/10.1016/j.enconman.2019.112449
[59] Unnikrishnan, K.S., Santhosh, K., Rohinikumar, B. (2024). Experimental and numerical analysis of PV-PCM integrated with novel shaped corrugated fins. Thermal Science and Engineering Progress, 50: 102562. https://doi.org/10.1016/j.tsep.2024.102562
[60] Kibria, M.G., Paul, U.K., Mohtasim, M.S., Das, B.K., Mustafi, N.N. (2024). Characterization, optimization, and performance evaluation of PCM with Al2O3 and ZnO hybrid nanoparticles for photovoltaic thermal energy storage. Energy and Built Environment, 6(6): 1118-1141. https://doi.org/10.1016/j.enbenv.2024.06.001
[61] Sun, A., Sun, Y.Z., Zhao, J.W., Song, X.Z. (2025). Characterization, experimental study and optimization of

the performance of photovoltaic panel integrated with form-stable phase change materials and conductive ZnO/MnO2 nanoparticles. Solar Energy Materials and Solar Cells, 292: 113752. https://doi.org/10.1016/j.solmat.2025.113752
[62] Azimi, N., Sharifzadeh, E. (2025). Using binary-eutectic phase change materials and ZnO/aluminum nitride nanofillers to improve photovoltaic efficiency. Solar Energy Materials and Solar Cells, 284: 113490. https://doi.org/10.1016/j.solmat.2025.113490
[63] Kibria, M.G., Mohtasim, M.S., Paul, U.K., Das, B.K., Saidur, R. (2024). Impact of hybrid nano PCM (paraffin wax with Al2O3 and ZnO nanoparticles) on photovoltaic thermal system: Energy, exergy, exergoeconomic and enviroeconomic analysis. Journal of Cleaner Production, 436: 140577. https://doi.org/10.1016/j.jclepro.2024.140577
[64] PraveenKumar, S., Agyekum, E.B., Kumar, A., Velkin, V.I. (2023). Performance evaluation with low-cost aluminum reflectors and phase change material integrated to solar PV modules using natural air convection: An experimental investigation. Energy, 266: 126415. https://doi.org/10.1016/j.energy.2022.126415
[65] Rubaiee, S., Fazal, M.A. (2023). Efficiency enhancement of photovoltaic solar system by integrating multi-pipe copper frame filled with ZnO-doped phase change material. MRS Energy and Sustainability, 10(2): 181-188. https://doi.org/10.1557/s43581-023-00063-1

NOMENCLATURE

A	Surface area of photovoltaic module, m²
G	Solar irradiance (solar radiation intensity), W/m²
P	Electrical power output of the PV module, W
Tpv	Photovoltaic module temperature, °C
Tamb	Ambient temperature, °C
h	Convective heat transfer coefficient, W/m²K
ηth	Thermal efficiency of the PV system, %
ηel	Electrical efficiency of the PV system, %
SMD	Standardized Mean Difference (effect size in meta-analysis)
I²	Heterogeneity index in meta-analysis, %
Q	Cochran's Q statistic
PCM	Phase Change Material
NePCM	Nano-Enhanced Phase Change Material
TES	Thermal Energy Storage
PV	Photovoltaic
PV–PCM	Photovoltaic system integrated with phase change material
PV–NePCM	Photovoltaic system integrated with nano-enhanced PCM
ZnO	Zinc Oxide nanoparticles
CNT	Carbon Nanotube
GO	Graphene Oxide
EG	Expanded Graphite
SEM	Scanning Electron Microscopy
TEM	Transmission Electron Microscopy
XRD	X-ray Diffraction
DSC	Differential Scanning Calorimetry
TGA	Thermogravimetric Analysis
PRISMA	Preferred Reporting Items for Systematic Reviews and Meta-Analyses